SOME APPLICATIONS OF AN OPTIMUM DESIGN TECHNIQUE TO FLAPPING WING DESIGNS

Koji Isogai †
Professor Emeritus, Kyushu University, Fukuoka, Japan

Flapping wing has been utilized in many engineering fields such as power generation, micro aerial vehicles, under water vehicles, etc.. As is well known, flapping wing motion is governed by many parameters such as frequency, heaving amplitude, pitching (or feathering) amplitude, phase difference between heaving and pitching motions for rigid wing and additional parameters such as bending and torsion rigidity, mass distribution, etc. for elastic wings. Therefore, the application of optimum design technique plays crucial role for the design of high performance devices/vehicles using flapping wing. In this paper, some applications of an optimization technique to the flapping wing designs that the present author has studied during last fifteen years of his career are outlined. They are a flutter power generation system, a micro aerial vehicle and its use for the estimation of the propulsive performance of dolphin.

Keyword: power generation, flapping wing MAV, propulsive efficiency of dolphin, optimum design

1. ELASTICALLY SUPPORTED FLAPPING WING POWER GENERATOR[1)]

In this section, the application of an optimization technique to a power generation system utilizing an elastically supported flapping wing power generator is explained. As shown in Fig. 1, a rigid rectangular wing is supported elastically in heaving oscillation while the pitching oscillation of the whole wing is mechanically driven by an electric motor with a prescribed frequency and amplitude. The basic idea of this system is that the lift induced by the pitching oscillation does work to the heaving oscillation while the phase angle between the two motions is automatically adjusted to the optimum value by aeroelastic response as shown later. (It can also be shown later that the work consumed by the forced pitching oscillation is less than 1% of the total energy generated by wind.)

1.1. METHOD OF ANALYSIS

The governing equation of motion of this system can easily be derived as follows:

$$M_h d^2H/dT^2 + \omega_h{}^2 M_h(1+ig)H = L + M_w(X_{cg} - A)d^2\alpha/dT^2 \qquad (1)$$

where T is time, H is the vertical displacement of the wing (positive up), α is the displacement (positive nose-up) of the forced pitching oscillation, M_h is the total mass relating to the heaving oscillation (including wing, electric motor, etc.), ω_h is the natural circular frequency of heaving oscillation, g is the artificial structural damping coefficient added to the system to maintain harmonic oscillation with constant amplitude, A is the location of the axis of pitch, X_{cg} is the location of the center of mass of the wing, M_w is the wing mass, and L is the lift (positive up). We assume here that the wing is designed so that the center of mass of the wing

†koji.isogai@nifty.com

coincides with the axis of pitch, namely, $X_{cg}=A$. With this assumption, the second term of the right hand side of Eq. (1) can be removed, which from our experience gives unfavorable effects on the power generation.

If we assume the aspect-ratio of the present rectangular wing is large, we can employ 2D unsteady (potential) aerodynamic forces, for that the analytical solutions are given, for solving Eq. (1). As a system of wind power generator, the designer should give the following parameters, those are, semi-chord length b, wing span l, the nominal free-stream velocity U and the amplitude of forced pitching oscillation α_o. From the dimensionless form of Eq. (1), it can be easily identified that the aeroelastic response of the system is also governed by the following five non-dimensional parameters: reduced frequency k ($b\omega/U$, ω: circular frequency of the forced pitching oscillation), g, ω_h/ω, mass ratio μ ($=M_h/(\pi\rho b^2 l)$, and a ($=A/b$). Once these parameters are given, it is easy to obtain, with the assumption of simple harmonic motion of the wing, the analytical solution of Eq. (1), namely, the amplitude and phase angle (with respect to the forced pitching oscillation) of the heaving oscillation. Then, it is easy to estimate the time averaged work done by the aerodynamic forces, namely, the wind energy extracted from the system. The problem is, however, how we can determine those parameters (five dimensionless parameters described previously) that give the highest power generation efficiency. The power generation efficiency η_p is defined by

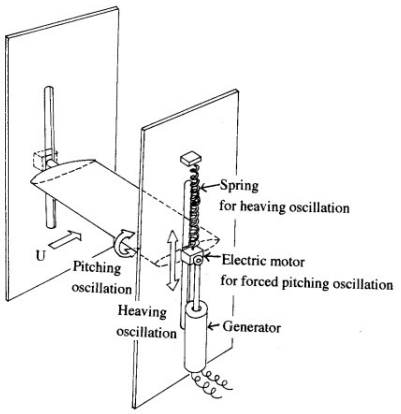

Figure 1 : Concept of elastically supported flapping wing power generator.

$$\eta_p = W/((1/2)\rho U^3(2H_s)l(16/27)) \qquad (2)$$

where W is the rate of work, the coefficient, 16/27, is referred as the Betz coefficient, and H_s is the amplitude of the leading or trailing edges, either of which is larger than the other. We employ an optimization algorithm "Complex Method", which is originally proposed by Box[2], to determine the five dimensionless parameters that attain the maximum efficiency.

1.2. APPLICATION OF OPTIMIZATION TECHNIQUE

We applied the Complex Method to the rectangular wing of aspect ratio 10 ($b=0.5m$ and span $l=10m$) with $\alpha_o=50$ *deg* in the nominal wind speed of *15 m/s*. The Complex Method is one of the optimization methods that do not depend on the derivatives of objective and constraint functions, and it can handle the multiple constraints. In the present study, the objective function is the power generation efficiency η_p, while the design variables are the five dimensionless parameters, namely, k, g, ω_h/ω, μ, and a. (It should be noted that x_{cg} is assumed to be equal to a.) We have imposed the following constraints to this problem:

$k<0.30$, $0.5<\mu<200.0$, $-1.0<a<1.0$, $0.5<\omega_h/\omega<1.5$,

$0.5<H_o/b<2.0$, $100\ deg<\phi<150\ deg$, $g>0.0$, $W>1\ kW$, $W_2<0.0$

where H_o is the amplitude of the heaving oscillation, ϕ is the phase delay angle of the heaving oscillation with

respect to the forced pitching oscillation, and W is the total power generated which is the sum of W_1 and W_2, where W_1 is the work done by lift and W_2 is the work done by pitching moment. Among these constraints, those imposed to μ, a, ω_h/ω and H_o/b are for that these variables should be within the practical range. The constraints imposed to k, ϕ and W_2 need some explanation. These constraints are imposed so that the dynamic stall phenomenon gives favorable effects on the power generation. According to our numerical simulations using a Navier-Stokes (NS) code, the dynamic stall phenomenon reduces both the efficiency and the power considerably if these constraints were not imposed. By applying these constraints to k, ϕ and W_2, it is guaranteed, as shown in Ref. 1, that the dynamic stall phenomenon increases both the efficiency and the power beyond those predicted by the present optimization code which employs the potential aerodynamics. What we have obtained by applying the present optimization code to the model system with the constraints described above is as follows:

η_p=49 %, W=6.99 kW, W_1=6.99 kW, W_2=-0.014 kW

The detailed values of other parameters obtained at this optimum condition are as follows: k=0.30, g=0.472, ω=9.0 rad/s, ω_h=8.06 rad/s, a=0.412,

μ=23.8, H_o=0.471m, ϕ=110 deg

It should be noted, however, that the maximum effective angle of attack for this case becomes about *34 deg*, which is far beyond the static stalling angle (NACA0012 airfoil section is assumed). Therefore, we also have performed the aeroelastic response computation of the present elastic system by using a 2D compressible Navier-Stokes code which have been developed by one of the present authors (see further details in Ref. 1).

1.3. EFFECT OF PLANFORM ON EFFICIENCY AND POWER

When the lift in Eq. (1) is replaced by that computed by 3D potential theory, namely, by doublet lattice method (DLM), we can evaluate the effect of the plan-form of the flapping wing. In this section, the comparison of the power and efficiency of the two different plan-forms, namely, a plan-form of a caudal fin of

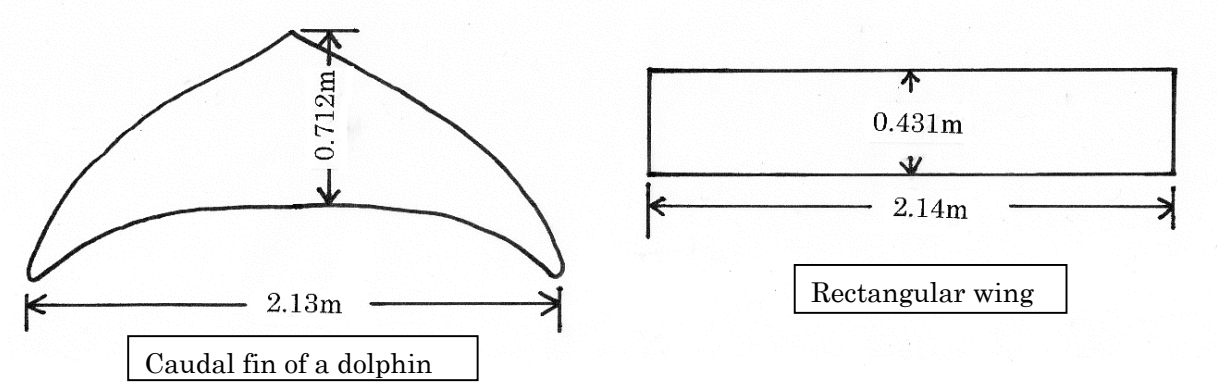

Figure 2 : Plan-forms used for the study of the flapping wing power generator.

a dolphin and a rectangular wing are discussed. The plan-forms are shown in Fig. 2. As shown in Fig. 2, the caudal-fin of dolphin has the root chord length of 0.712 m, the full span length of 2.13 m and the wing area of 0.922 m^2 and the aspect-ratio of 4.96. The rectangular wing has the same wing area and aspect ratio as those of the dolphin tail. The both wing has the same wing section of NACA0015 and are assumed to be operated in

the water with velocity of 2 m/s. The same optimization technique discussed in section 1.2 is applied to these systems to determine the elastic and mass properties of each system to obtain the maximum efficiency. As a result, the power and efficiency obtained for the caudal fin of the dolphin are 984 W and 20 %, respectively, with k=0.30, H_o=0.37 m, θ_o=50 deg and ϕ=89 deg, and the power and efficiency for the rectangular wing are 1,009 W and 34 %, respectively, with k=0.30, H_o=0.224 m, θ_o=50 deg and ϕ=90 deg. From these results we can conclude that the rectangular wing shows better performance than the dolphin type plan-form. To examine the effect of viscosity, the numerical simulations for the same optimized systems using the 3D Navier-Stokes code were conducted. As the results, the power and efficiency of the dolphin type plan-form are 726 W and 14.7 %, respectively while those of the rectangular wing are 1,070 W and 36.1 %, respectively. Therefore, the power and efficiency of the rectangular wing are increased by the viscous effect, namely, the dynamic stall effect, while those of the dolphin type plan-form is decreased from those predicted by the potential theory. Therefore as far as we concern about the flapping wing power generator, we can conclude that the rectangular plan-form is superior compared with the dolphin type plan-form.

1.4. EXAMPLES OF A 2 DIMENSIONAL MULTI-WING CASCADE CONFIGURATION[3)]

The analytical method for two-dimensional (2D) multi-wing cascade configuration of the elastically supported flapping wing power generator was also developed (details of the analysis using the doublet lattice method should be referred to Ref. 3). The same optimization technique as used for a single wing configuration described in section 1.2 is applied to the middle wing of a 2D three wing cascade configuration. The following assumptions are made for a design study: wing chord is 1 m; wing distance between the adjacent wings is 2.0 m; amplitude of the forced pitching oscillation is 50 deg; oscillation mode is anti-phase; wind speed is 8 m/s. The results of optimization are as follows: power is 132 W/m, η_p=50.3 % (C_p=0.30). The power and efficiency of the outer two wings are 111 W/m, η_p=42.6% (C_p=0.25). Therefore the total power of three wings of span 10 m is 3.54 kW. (C_p is defined as power coefficient.)

1.5. EXAMPLES OF A 3 DIMENSIONAL MULTI-WING CASCADE CONFIGURATION

The analytical method for a rectangular multi-wing cascade configuration of the elastically supported flapping wing power generator was also developed (details of the analysis using the doublet lattice method should be referred to Ref. 4). The same optimization technique as used for a single wing configuration described in section 1.2 is applied to the middle wing of a rectangular three wing cascade configuration which is assumed to be used in the water channel. The following assumptions are made for a design study: wing chord is 0.431 m; full span is 2.14 m; area is 0.922 m^2; aspect ratio is 4.96; wing distance between the adjacent wings is 0.65 m; amplitude of the forced pitching oscillation is 50 deg; oscillation mode is anti-phase; water velocity is 2 m/s. The results of optimization are as follows: power of the middle wing is 1.45 kW, η_p=41.2 % (C_p=0.244). The power and efficiency of the outer two wings are 1.30 kW, η_p=36.7 % (C_p=0.217). Therefore the total power of three wings is 3.85 kW. Therefore, total power generated during one month for this system becomes $3.85 \times 0.80 \times 24 \times 30 = 2,219$ kWh/month. Since the average power needed for one standard family is about 373.5 kWh, the present hydro-power generator of 3 wing configuration can supply the power needed by about 6 standard families.

2. APPLICATION OF OPTIMIZATION TECHNIQUE TO RESONANCE TYPE FLAPPING WING[5)]

In this section, the application of the optimization technique to a resonance type flapping wing for a dragonfly-type micro aerial vehicle, which shows high performance in spite of its simple structure and light weight, is briefly explained. Figure 3 shows the planform and structure of the present resonance type flapping wing. The experimental and numerical studies (using a 3D NS code) on the single/tandem wing configurations using this original resonance type flapping wing have been conducted. Figure 4 shows the arrangement of tandem wing configuration. Figure 5 shows the variation of lift under hovering condition with respect to the oscillation frequency. As seen in Fig. 5, the agreement between the numerical and experimental results is very good for a single wing configuration in the frequency range between 35 Hz to 50 Hz. In Fig. 5, the results obtained using the 3D NS code for the tandem wing configuration are also shown. In this case, the phase difference ψ between the flapping wing motions of the fore- and hind-wings is assumed to be zero. As seen in the figure, the lifts generated by the fore- and hind-wings increase about 25 % at f=50Hz compared with that of the single wing configuration. It is clear that this increase of lift is due to the flow interaction between the two wings. The efficiency $\overline{P}/\overline{L}$

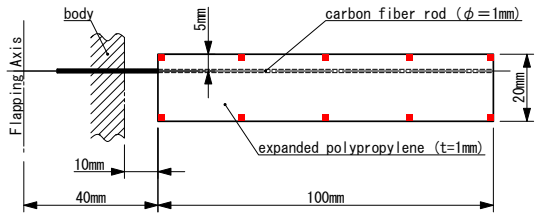

Figure 3 : Planform, arrangement and structure of resonance type flapping wing.

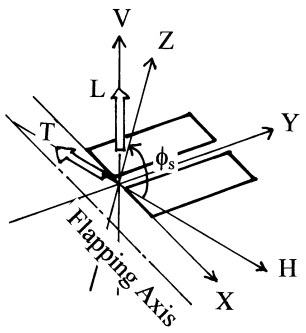

Figure 4 : Arrangement of tandem wing configuration.

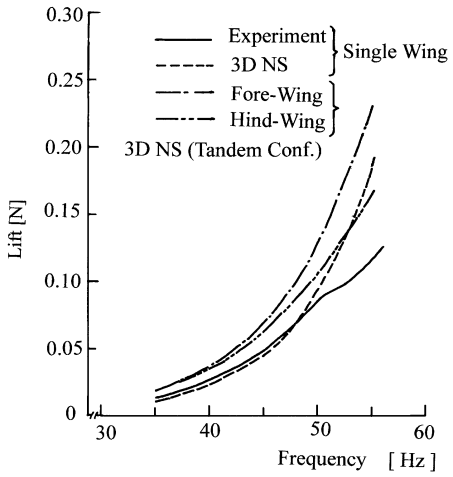

Figure 5 : Lift vs. frequency characteristics.

(necessary power per unit lift) at f=50 Hz for the tandem wing configuration is 22.0 W/N. The original structure of the resonance type flapping wing shown in Fig.3 is not necessarily the optimum structure which gives the highest efficiency. Therefore we try to determine the optimum diameter of the CFRP rod and the thickness of the EPP plate of the present resonance type flapping wing. The planform and the arrangement of the CFRP rod and the EPP plate are assumed to be same as the original wing (see Fig. 3). For this purpose, we have developed the optimization code which couples the optimization algorithm, vibration analysis code and

the 3D NS code. As to the optimization algorithm, the Complex Method[2], which is one of the direct search method without recourse to the derivatives, is also employed. The objective function of the present problem is the efficiency, namely, $\overline{P}/\overline{L}$. We have employed total five design variables, that are, the diameter of the CFRP rod (d), the thickness of the EPP plate (h), the flapping amplitude (ϕ_o), the reduced frequency (k) and the stroke-plane angle (ϕ_s). The constraint is that the time mean lift ($\overline{L}$) should be larger than the weight of the MAV. The weight of the MAV is assumed to be 0.392 N (40 gf). Since the number of the design variables is only five, we have obtained the converged solution after 8 iteration steps. The results of the optimization are as follows: $\overline{P}/\overline{L}$=10.8 W/N ($\overline{L}$=0.460 N, $\overline{P}$=4.97 W), d=1.93 mm, h=1.16 mm, k=0.541 (f=52.42 Hz), ϕ_s=-4.5 deg. The theoretical natural frequencies of the optimized wing are f_1=83.0 Hz, f_3=115 Hz and f_4=3,788 Hz. The efficiency of the present optimized wing, namely, $\overline{P}/\overline{L}$=10.8 W/N is the improvement of 51% over the 22.0 W/N of the original wing. The theoretical values of d and h of the original wing are d=1.65 mm and h=1.95 mm. (It should be noted that these values of d and h of the original wing are adjusted so that the theoretical natural frequencies match with those of the ground vibration test data.) When we compare the values of d and h of the optimized wing with those of the original wing, it is identified that the stiffness of the CFRP rod is increased while the stiffness of the EPP plate is reduced considerably for the optimized wing compared with those of the original wing. This fact enables the larger feathering displacement of the optimized wing than that of the original wing as confirmed in Figs. 6, which show the aeroelastic responses at the tip stations of the fore- and hind-wings in hovering condition.

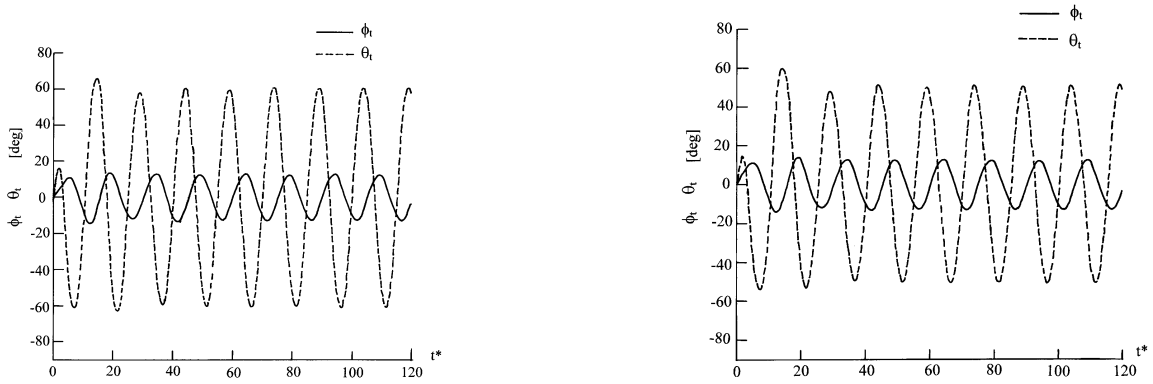

(a) Fore-wing (b) Hind-wing

Figure 6 : Aeroelastic responses for optimized fore- and hind-wings.

3. PROPULSIVE PERFORMANCE OF DOLPHINE

In this section, the application of an optimization technique to the analysis of propulsive performance of dolphins is outlined. (Details of the analyses should be referred to Ref. 6 and 7.) In a paper published in 1936, Gray[8] pointed out that the power generation capability of a dolphin's muscle is seven times larger than that of a terrestrial mammal. This conclusion was derived on the basis of the assumptions that the maximum speed of

the dolphin is 20 knots (10 m/s), that the friction drag of the body can be estimated by assuming that the boundary layer around the body is turbulent and that the propulsive efficiency is 100%. If these assumptions are correct, the conclusion he derived is contradictory to the fact that the dolphin is a mammal. Therefore, it is called “Gray’s paradox.” Gray also pointed out in the same paper that the power generation capability of a dolphin’s muscle might be equivalent to that of other types of mammalian muscle if the boundary layer around the body is laminar. Numerous studies have been made on the nature of the boundary layer since then (see the extensive review by Fish and Rohr[9]). However, Fish[10] concluded, by examining the numerous studies on the nature of the boundary layer, that there is no special mechanism for drag reduction and dolphins appear to maintain a turbulent boundary layer. Fish computed the thrust, efficiency and power using a potential theory from the experimental data of the fin motion read from video footage of several trained dolphins swimming horizontally. Then he computed the drag coefficient from the computed power. However, the value of the drag coefficient and the power thus derived show considerable scatter depending on the data of the individual dolphin used for the analyses, making the accurate determination of the power generation capability of dolphins difficult. (The power thus determined around the maximum speed of 6 m/s was scattered from 1,900 W to 7,600 W.) On the other hand, there is no such uncertainty for the standing swimming performance shown in aquariums where the body (in the air) is supported by the caudal fin in the water (see Fig. 7). It is clear that the thrust generated by the fanning motion of the caudal fin is equal to the body weight, which can be measured accurately. Therefore, an accurate estimation of the power generation capability could be possible without having to include the body drag if we can analyze the standing swimming. An analysis of standing swimming is only possible using a numerical simulation technique which takes into account the effect of viscosity, since the flow around the caudal fin becomes an unsteady viscous flow with large scale flow separation. As the first step, we determine the power necessary for the standing swimming using a three-dimensional Navier–Stokes (3D NS) code. To the best of our knowledge, no analysis of standing swimming has been published to date. As the next step, we estimate the maximum speed in water based on the power generation capability thus determined. For the analysis of the second step, we employ a 3D modified doublet lattice method (MDLM) (modification of the doublet lattice method taking into account leading edge suction) coupled with an optimization technique. As will be discussed later, the optimization method is used to find the optimum fin motion which attains the maximum propulsive efficiency.

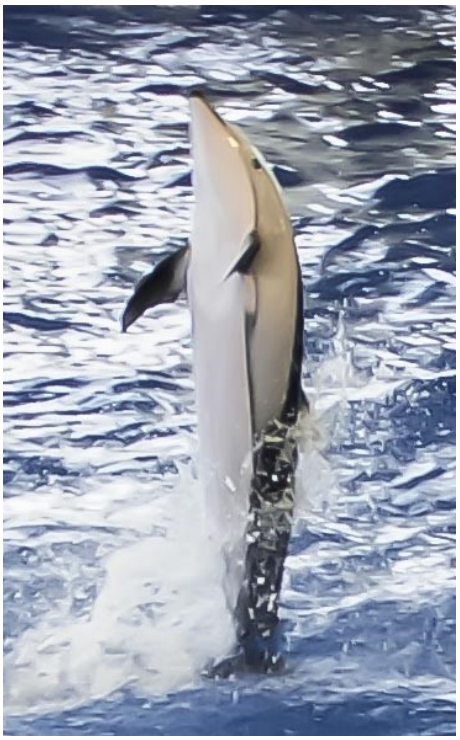

Figure 7 : Standing swimming of a dolphin.

3.1 MOEL DOLPHIN AND METHOD OF ANALYSIS

In the present analysis, we consider one of the bottlenose dolphins (*Tursiops truncates*) studied by Nagai[11] for the analytical model. The length (l), mass (M) and fineness ratio (l/d, d: maximum diameter of body) of the model dolphin are 2.3 m, 138 kg and 5.38, respectively. Figure 8 shows the planform of the caudal fin. The root chord length is 0.144 m, the full span length is 0.432 m and the area of the fin is 0.0377 m^2. The aspect ratio is 4.96. The airfoil section of the fin is assumed to be NACA0021. In this analysis, the flexibility of the caudal fin is also taken into account.

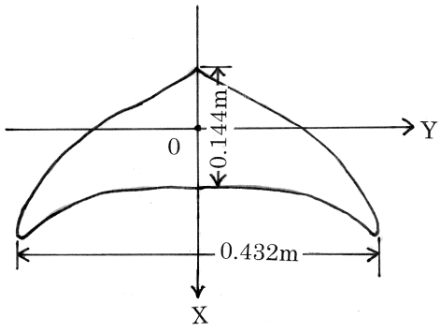

Figure 8 : Plan form of caudal fin.

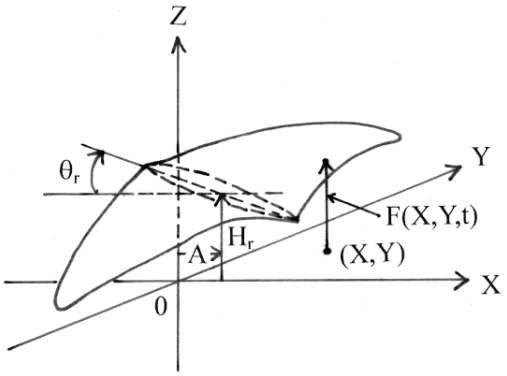

Figure 9 : Definitions of coordinate and fin motion.

The elastic property of the fin such as Young's modulus is taken from the data reported by Sun et al.[12]. For hydro-elastic response computations, we apply the modal approach used in Ref. 5. Figure 9 shows the definitions of the coordinates and the fin motion. In the modal approach, the displacement of the fin mean surface $F(X,Y,t)$ in the Z direction is expressed using nine mode shapes as

$$F(X,Y,t) = F_r(X,Y,t) + \sum_{i=1}^{9} \phi_i(X,Y) q_i(t) \qquad (3)$$

where $F_r(X,Y,t)$ is the rigid displacement due to the forced oscillation, $\phi_i(X,Y)$ is the i-th natural vibration mode of the fin and q_i is the unknown generalized coordinate of the elastic deformation. The rigid displacement $F_r(X,Y,t)$ of the fin can be expressed as

$$F_r(X,Y,t) = H_r - (X-A)\theta_r \qquad (4)$$

where H_r and θ_r are the heaving and pitching displacements, respectively, and they are given as

$$H_r = H_o \sin(\omega t) \qquad (5)$$

$$\theta_r = \theta_o \sin(\omega t + \phi) \qquad (6)$$

where H_o and θ_o are the amplitudes of the heaving and pitching oscillations, respectively, ω is the circular frequency of forced oscillation and ϕ is the phase advance angle of the pitching oscillation ahead of the heaving oscillation. Using Lagrange's equations of motion, we obtain the ordinary differential equations of motion to determine q_i as follows.

$$M_i(d^2 q_i / dt^2) + (\omega_i^2 / \omega) g M_i dq_i / dt + \omega_i{}^2 M_i q_i = -\iint_S m(X,Y)\phi_i(X,Y)(d^2 F_r / dt^2) dXdY + \iint_S \Delta P(X,Y,t)\phi_i(X,Y) dXdY$$

for i=1,……., 9 (7)

where M_i is generalized mass, ω_i is the i-th natural circular frequency, $m(X,Y)$ is mass per unit area of fin, $\Delta P(X,Y,t)$ is the pressure difference between the upper and lower surfaces of the fin and g is the damping coefficient which is equivalent to the structural damping coefficient. Equations (3)–(7) are the basic equations for computing hydro-elastic deformation of the flexible fin, those are used both for the NS simulations including the standing swimming and the horizontal swimming.

3.2 RESULTS OF STANDING SWIMMING

For the numerical simulation of the standing swimming, the 3D NS equations are solved with Eq. (7). The 3D NS code used in the present study is a Reynolds averaged Navier–Stokes (RANS) code originally developed by Isogai. (See Ref. 7 for further details of the analysis.)

In Fig. 10, the flow pattern (stream lines) around the 52% semispan at the typical phase of oscillation is shown. As seen in the figure, large-scale flow separation around the leading edge region is observed. As the result of the numerical simulation, we obtain the time-averaged thrust of 1,352 N (138 kgf) which can sustain the body weight of 138 kgf with the necessary power of 8,582 W. These results give power-mass-ratio (PMR: power per unit mass of body) of 62.2 W/kg which is 2.6 times larger than that of a human athlete and it is an approximately 11% reduction compared with 70.2 W/kg which was obtained under the assumption of the rigid fin [6].

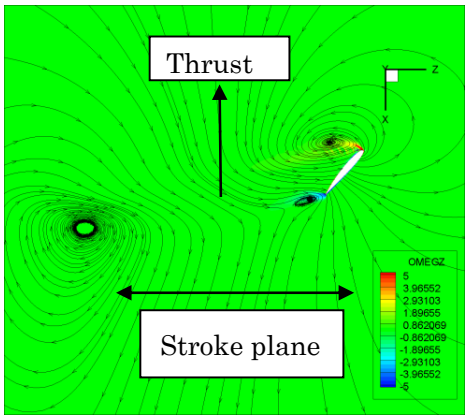

Figure 10 : Flow pattern around the 52% semispan for the standing swimming condition.

It is of great interest to determine the maximum swimming speed of the present model dolphin when the power predicted by the standing swimming is used for horizontal swimming in water. This analysis is presented in the next section.

3.3 RESULTS OF HORIZONAL SWIMMING

In this section, the propulsive performance of horizontal swimming of the present model dolphin is estimated using the MDLM coupled with an optimization technique[2]. The optimization technique is used to find the optimum fin motion which attains the maximum propulsive efficiency. As the result of optimization, the thrust, power, propulsive efficiency and PMR at the optimum condition are determined. In order to evaluate the effect of the viscosity, especially the effect of flow separation, on the performance thus determined using the MDLM, the numerical simulations using the 3D NS code are also conducted. (Details of the procedure of computing the performance of horizontal swimming should be referred to Ref. 6 and 7.)

The propulsive performance of the horizontal swimming at the speeds of V=6.5 m/s, 9.43 m/s, 11 m/s and 12 m/s is shown in Fig. 11, where the results obtained using the MDLM are shown by the solid line and the results obtained using the 3D NS code are shown by the solid circles. As seen in the figure, the PMR predicted by the 3D NS code is larger; namely, approximately 16% for V=6.5 m/s and 21% for V=12 m/s, than that

predicted by the MDLM. These discrepancies between the two can be attributed to the effect of flow separation observed at the tip region.

From Fig. 11, it is identified that the maximum speed of horizontal swimming is estimated as 12 m/s. Note that the PMR of the maximum speeds of dolphins observed in the aquariums, namely, 6.5-9.5 m/s, are in the range 10–30 W/kg, far below the PMR of 62.2 W/kg estimated from the analysis of the standing swimming.

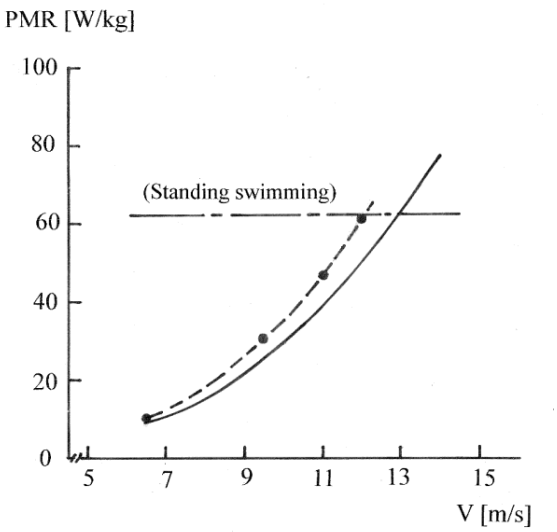

Figure 11 : Variation of PMR with respect to horizontal speed.
(3D NS: ● , MDLM: ———).

REFERENCES

1) Isogai, K, Yamamoto, M., Matsubara, M. and Asaoka, T. : Design study of elastically supported slapping wing power generator, International Forum on Aeroelasticity and Structural Dynamics, Amsterdam, 2003.
2) Box, M. J. : A new method of constrained optimization and a comparison with other methods", *Computer Journal*, Vol. 8, pp. 42-52, 1965.
3) Isogai, K. and Abiru, H. : Study of multi-wing configurations of elastically supported flapping wing power generator, *Trans. Jpn. Soc. Aeronaut. Space Sci.*, 55, No. 2, pp. 133-142, 2012.
4) Isogai, K. and Abiru, H. : Lifting-surface theory for multi-wing configurations of elastically supported flapping wing power generator, *Trans. Jpn. Soc. Aeronaut. Space Sci.*, 55, No. 3, pp. 157-165, 2012.
5) Isogai, K. and Nagai, H. : Experimental and numerical study of resonance type flapping wings for micro aerial vehicles, APISAT 2009, Nov. 4-6, 2009.
6) Isogai, K. : Propulsive performance of dolphins –Estimation from analysis of standing swimming-, *Trans. Jpn. Soc. Aeronaut. Space Sci.*, 56, No. 2, pp. 90-95, 2013.
7) Isogai, K. : Effect of flexibility of the caudal fin on the propulsive performance of dolphins, *Jpn. Soc. Aeronaut. Space Sci.*, 57, No. 1, pp. 21-30, 2014.
8) Gray, J. : Studies in animal locomotion. VI. The propulsive powers of the dolphin, *J. of Experimental Biology* **13**, pp.192-199, 1936.
9) Fish, F. E. and Rohr, J. J. : Review of dolphin hydrodynamics and swimming performance, *SSC San Diego*, Technical Report 1801, 1999.
10) Fish, F. E. : Power output and propulsive efficiency of swimming bottlenose dolphin (*Tursiops truncates*), *Journal of Experimental Biology,* **185** , pp. 179-193, 1993.
11) Nagai, M. : *Thinking fluid dynamics with dolphins*, Ohmsha Press, 2002.
12) Sun, Q., Morikawa, H., Kobayashi, S., Ueda, K., Miyahara, H. and Nakajima, M. : Structure and mechanical properties on tail flukes of dolphin, *J. of Aero Aqua Bio-Mechanisms*, **1,** No. 1, 2011.

Prof. Emeritus

Koji Isogai (Kyushu University, Japan)

Koji Isogai graduated the graduate course of the Department of Aeronautics of Kyushu University, Japan in 1965. He entered the National Aerospace Laboratory (Japan) in 1965, where he conducted the research works on the aeroelasticity and unsteady aerodynamics of aircraft for 28 years. He moved to the Department of Aeronautics and Astronautics of Kyushu University in 1993, then he moved to the Department of Aeronautics and Astronautics of Nippon Bunri University in 2004 and he retired in 2010. He is now Professor emeritus of Kyushu University. He is the honorary member of The Japan Society for Aeronautics and Space Sciences and the Associate Fellow of American Institute of Aeronautics and Astronautics. He has published about 90 papers in refereed journals and in full paper conference proceedings. His research fields are the transonic aeroelasticity of aircraft, flapping wing power generator, unsteady fluid dynamics of bird, insect and fish, and micro aerial vehicle (MAV).